The Hinge Region Regulates DNA Binding, Nuclear Translocation, and Transactivation of the Androgen Receptor

Annemie Haelens, Tamzin Tanner, Sarah Denayer, Leen Callewaert, and Frank Claessens

Molecular Endocrinology Laboratory, Department of Molecular Cell Biology, Faculty of Medicine, Campus Gasthuisberg, University of Leuven, Leuven, Belgium

Abstract

The androgen receptor (*AR*) encoding gene can undergo mutations during the development and treatment of prostate cancer. Even in hormone-independent stages, mutations in the receptor paradoxically seem to result in an increased AR function. Two such point mutations have been described in the part of the AR involved in DNA binding and nuclear translocation, namely the hinge region. Despite a decreased nuclear translocation, these mutant ARs display increased transactivating potencies. Through detailed analysis of the hinge region, we found that deletion of residues 629 to 636 resulted in a stronger androgen response on different reporters, although this mutant displays an extremely low *in vitro* affinity for androgen response elements. This superactivity is independent of nuclear localization and can be inhibited by antiandrogens. Surprisingly, the AR activation functions, AF1 and AF2, are not dramatically affected when the inhibitory region (629-RKLKKLGN-636) is deleted, although cotransfected p160 coactivator TIF2 had a stronger potentiating effect in the absence of this motif. The ligand-dependent interaction between the amino-terminal domain and the ligand-binding domain (N/C interaction) plays an important role in transactivation by the AR. We found that this interaction is strongly enhanced by deletion of the inhibitory region. In conclusion, the description of prostate cancer mutations has led to the discovery of a complex role of the hinge region in nuclear localization, DNA binding, coactivator recruitment, and N/C interaction of the AR. [Cancer Res 2007;67(9):4514–23]

Introduction

The androgen receptor (AR) mediates the biological effects of androgens. These are responsible for the development of the male reproductive tissues and male secondary sex characteristics, and are essential for spermatogenesis (1). The AR not only plays a crucial role in the initiation and growth of prostate cancer but also in the response to androgen ablation and antiandrogen therapy (2–5). The benefits of these therapies are temporary because all patients eventually relapse, which coincides with an evolution from hormone-dependent to hormone-independent tumor growth. It seems that the AR may also be a key role player in this transition (2–5). It has been documented that in hormone-independent cancers, the *AR*-encoding gene could have undergone alterations such as amplification or mutation, or there can be an altered expression of coregulators (4). As a result, the cells are more sensitive to lower concentrations of hormone, respond to a broader range of ligands, or can be activated by other signaling pathways (4). Interestingly, several point mutations in and around the hinge region have been identified in prostate cancer patients (6–11).

The AR belongs to the superfamily of the nuclear receptors that are characterized by a highly conserved DNA-binding domain (DBD; ref. 12). Nuclear receptors have a canonical structure consisting of a highly variable amino-terminal domain (NTD) containing a ligand-independent transcription activation function 1 (AF1), the DBD, and a carboxy-terminal ligand-binding domain (LBD) with a ligand-dependent transcription activation function 2 (AF2). The DBD and the LBD are separated by a nonconserved and flexible hinge region (12).

Androgens enter the cell by passive diffusion through the cell membrane and bind to the AR, which resides in the cytoplasm in an inactive form due to the association with multiprotein complexes of chaperones (13). After ligand binding, the receptor dissociates from the chaperones and rapidly converts to an active form in which the NTD intramolecularly interacts with the LBD (14). This is followed by nuclear translocation, dimerization, and binding to androgen responsive elements (ARE) from which the receptor directs the transcription of androgen-regulated genes by the recruitment of coactivators (13–15).

Unlike other nuclear receptors, the AR AF2 is almost not active, probably because the AR AF2–coactivator interactions are weaker if compared with, for example, the estrogen receptor (16). Instead, AF1 is the major transactivation function of the AR, and the AR-NTD is the main recruiting surface for coactivators (16, 17). In addition, the AF2 coactivator recruitment surface of the AR is the primary interaction site for the NTD (18–20). It is the 23-FQNLF-27 motif in the AR-NTD that occupies the hydrophobic cleft in the LBD (21, 22). This interaction is functionally important because deletion of the 23-FQNLF-27 motif diminishes AR activity on some reporters (21) and is necessary for the induction of chromatin-based templates (23).

Initially, the hinge region of nuclear receptors was considered to be a flexible linker between the DBD and the LBD, allowing proper DNA binding and dimerization (24). However, for the AR, the hinge region turned out to be a multifunctional domain involved in DNA binding (25–28) and nuclear translocation (29). The AR-DBD consists of two zinc coordinating modules. It requires a carboxy-terminal extension (CTE) of at least 12 residues (625-TLGARKLK-KLGN-636) for optimal binding to androgen-selective AREs in bandshift assays (25–28). The hormone-dependent nuclear translocation is mainly mediated through a bipartite nuclear localization signal (NLS) consisting of two clusters of basic residues that are located in the DBD and the hinge region (29). The AR can also be acetylated in its hinge region at residues K630, K632, and K633 (30). Acetylation of these residues has been reported to regulate

Note: A. Haelens and L. Callewaert are postdoctoral fellows of the "Fonds voor Wetenschappelijk Onderzoek-Vlaanderen."

Requests for reprints: Frank Claessens, Campus GHB O/N Room 901, Herestraat 49, 3000 Leuven, Belgium. Phone: 32-16-330253; Fax: 32-16-345995; E-mail: frank.claessens@med.kuleuven.be.

doi:10.1158/0008-5472.CAN-06-1701

transcriptional activity (30, 31), subcellular distribution, and folding of the AR (32), coactivator and corepressor binding (31–33).

Two somatic point mutations in the hinge region of the human *AR* gene have been identified (6, 7). A R629Q mutation was isolated from a patient with androgen-independent prostate cancer after androgen ablation therapy. A K630T substitution was identified in a prostate cancer patient before the onset of androgen ablation therapy (7). In this report, we aimed to determine the effect of the two identified point mutants on the roles of the hinge region. Such insight could provide valuable information for the development of new therapeutic strategies to be used in the treatment of prostate cancer.

Materials and Methods

Materials. Restriction and modifying enzymes were obtained from Invitrogen, MBI Fermentas GmbH, Roche Molecular Biochemicals, and Takara Shuzo Co., Ltd. Oligonucleotides were purchased from Sigma-Aldrich.

Plasmid constructs. The pSG_5-flag plasmid was created by the insertion of three flag tags as an *Eco*RI/*Bam*HI PCR fragment into the empty pSG_5 plasmid (34). The human AR cDNA from the $pSVAR_o$, a kind gift of A.O. Brinkmann (Erasmus Medical Center Rotterdam, Rotterdam, the Netherlands), was cloned into the pSG_5-flag to obtain the wild-type (WT) construct. The AR mutants were created by two-step PCR site-directed mutagenesis. The SV40NLS-WT and SV40NLS-Δ11 expression plasmids were created by insertion of an oligonucleotide expressing the SV40 NLS (PKKKRKVD) in the pSG_5-flag plasmid. Subsequently, the cDNA fragments coding for either WT or Δ11 were inserted as *Bam*HI fragments into the *Bam*HI site of this SV40NLS pSG_5-flag construct. The pCMV-β-gal expression plasmid was obtained from Stratagene. The mouse mammary tumor virus (MMTV) luciferase reporter plasmid was a kind gift of Dr. P. Chambon (Institut de Génétique et de Biologie Moléculaire et Cellulaire, College de France, Illkirch, France). The SC ARE, C3(1) ARE, TAT GRE, and PB-ARE2 oligonucleotide luciferase reporter constructs are described earlier (35–37). The prostate-specific antigen (PSA) promoter luciferase reporter was obtained from D.J. Tindall (Department of Urology Research, Mayo Clinic, Rochester, MN). The enhanced green fluorescent protein (EGFP)-WT was a kind gift of K.E. Knudsen (Department of Cell Biology, University of Cincinnati, College of Medicine, Cincinnati, OH) and codes for the WT human AR NH_2-terminally fused to a red-shifted variant of GFP (EGFP). The EGFP-hinge mutants were created by replacing part of the human AR cDNA, including the hinge region by the corresponding mutant fragment. The $(GAL4)_5$TATA-luc luciferase reporter plasmid was a kind gift of M.G. Parker (Imperial Cancer Research Fund, London, United Kingdom). The $pUAS_4$-TATA-luc was described elsewhere (38). The expression vector for TIF2 (pSG_5-TIF2) was obtained from Dr. H. Gronemeyer (Institut de Génétique et de Biologie Moléculaire et Cellulaire, College de France Illkirch). The WT/ΔAF2 and Δ1/ΔAF2 plasmids code for a flag-tagged fusion protein consisting of the NH_2-terminal part of the AR (residues 1–662) with the GAL4 DBD (residue 1–147). The ΔAF1/WT plasmid codes for the human AR fragment (residues 550–919), NH_2-terminally fused to the GAL4 DBD (residues 1–147). The ΔAF1-hinge mutants were created by exchanging *Hin*dIII/*Psy*I inserts. VP16-NTD and VP16-ΔFQNLF are pSNATCH-II constructs described earlier as hAR_{1-529} and hAR_{1-529}ΔFQNLF (16, 21). The ΔFQNLF plasmid was described before

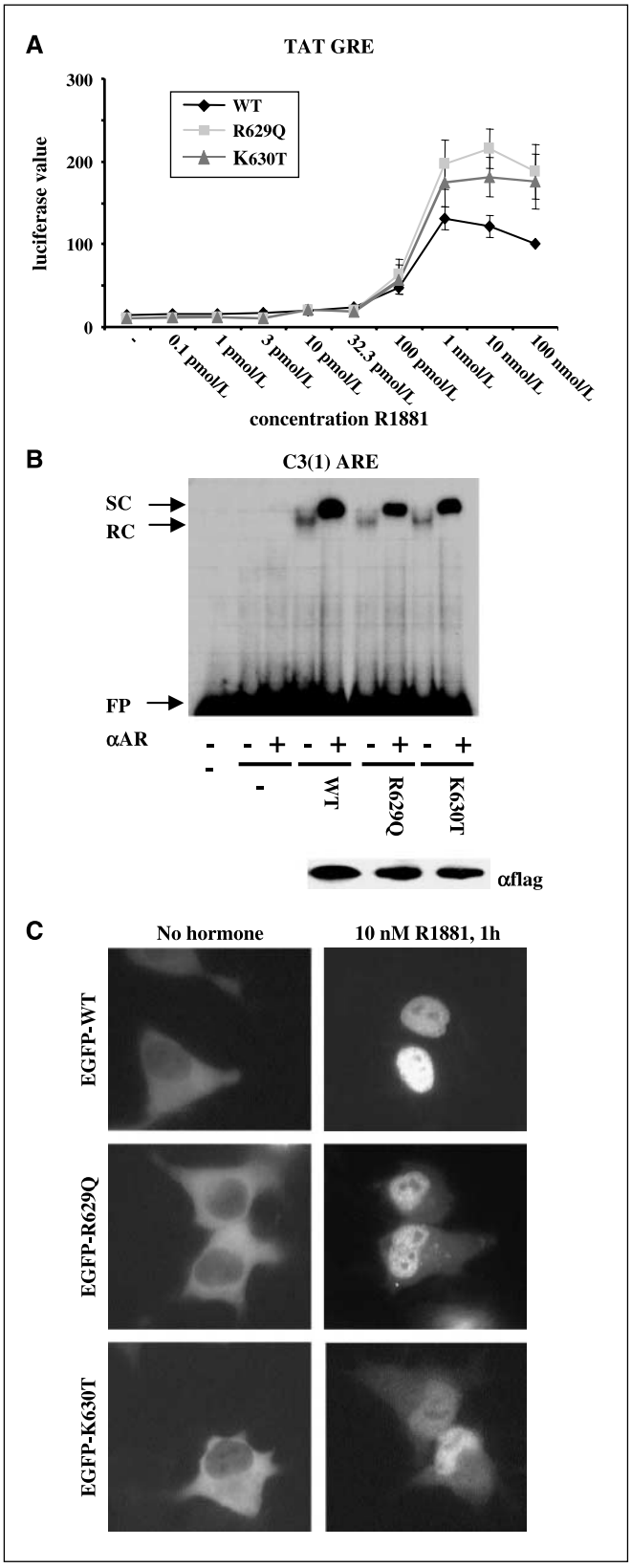

Figure 1. Analysis of two AR mutants R629Q and K630T. *A,* functional analysis. The expression plasmids for the WT and the mutant constructs R629Q and K630T were transfected into HeLa cells together with TAT GRE androgen-responsive reporter. The cells were stimulated for 24 h with different concentrations of R1881. The luciferase value of WT after 24-h stimulation with 100 mmol/L is set at 100%. *Bars,* SEM. *B,* DNA-binding analysis. The bandshift experiments were done by incubating the labeled C3(1) ARE probe with whole-cell COS extracts expressing the indicated construct. Equal expression was checked by immunoblotting. Extracts of nontransfected cells were added to the first lanes as a negative control. The supershifts were obtained by adding a specific antibody against AR (*αAR*). *Arrows,* positions of the free unbound probe (*FP*), the retarded complex (*RC*), and the supershifted complex (*SC*). *C,* fluorescence microscopy. HeLa cells were transfected with EGFP-WT, EGFP-R629Q, or EGFP-K630T expression plasmid. The subcellular distribution of the EGFP fusion proteins without hormone stimulation and after 1-h stimulation with 10 nmol/L R1881 was analyzed by fluorescence microscopy.

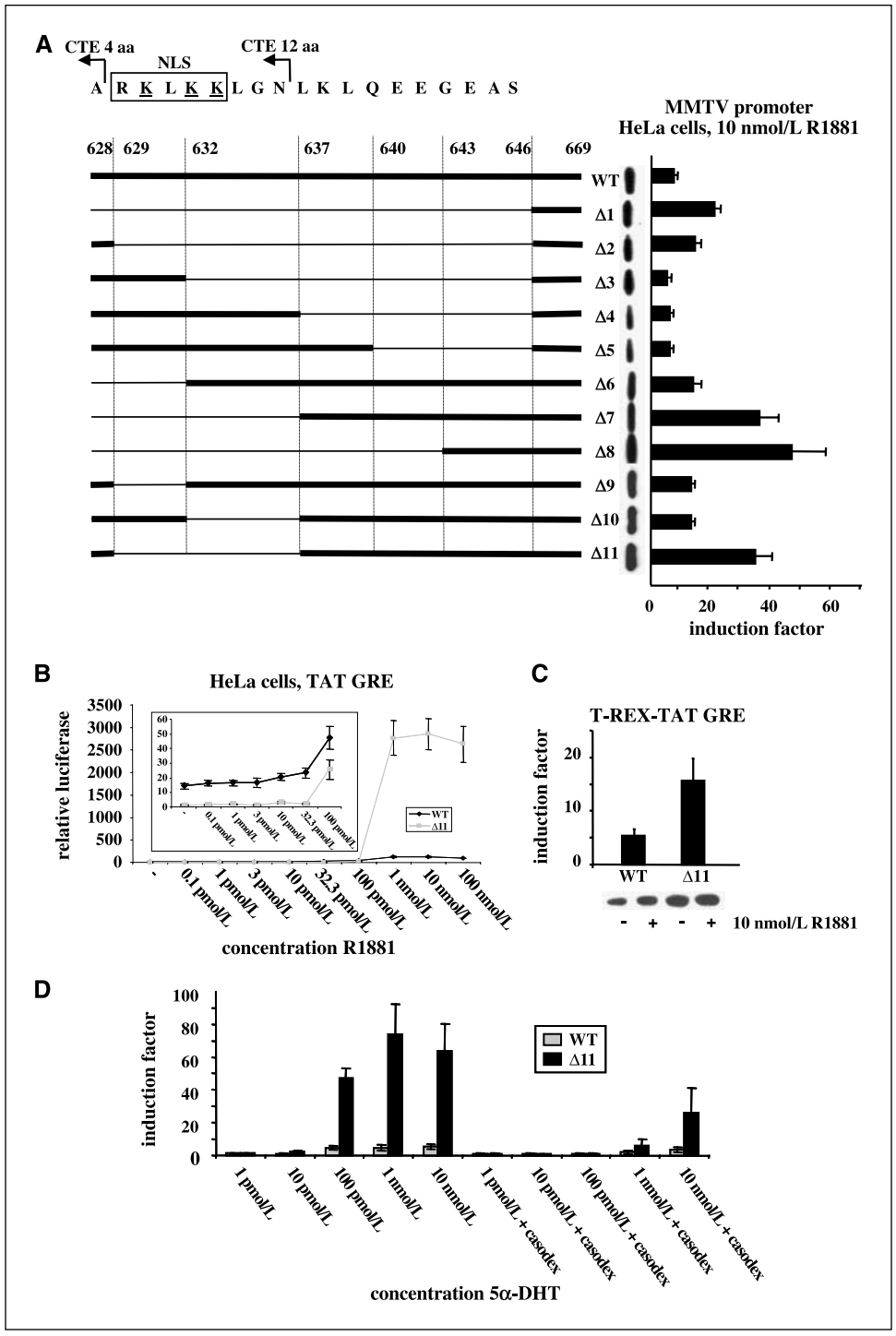

Figure 2. Identification and delineation of the inhibitory region. *A,* the hinge region of the AR. The protein sequence of the NH_2-terminal part of the hinge from amino acid 628 to 646 is shown. *Arrows,* the borders of the CTE required for binding to nonselective AREs (*CTE4*) and androgen-selective AREs (*CTE12*). The second half of the bipartite NLS (*boxed*) and the potential acetylation sites (*underlined*) are shown. For the functional analysis, HeLa cells were transfected with expression plasmids for WT and mutant ARs Δ1 to Δ11, together with the androgen-responsive MMTV luciferase reporter constructs. The cells were stimulated for 24 h with 10 nmol/L R1881. The results are shown as induction factor. *Bars,* SEM. For immunoblotting, the expression plasmids were transfected into HeLa cells, which were later stimulated for 1 h with 10 nmol/L R1881. The expressed proteins were detected using the anti-flag M2 antibody. *B,* the expression plasmids for WT and Δ11 were transfected into HeLa cells together with the TAT GRE luciferase reporter. The cells were stimulated for 24 h with different concentrations of R1881. The luciferase value of WT after 24-h stimulation with 100 mmol/L is set at 100%. *Bars,* SEM. *C,* T-REX-TAT cells were transfected with 50 ng WT or Δ11 expression plasmid and stimulated with 10 nmol/L R1881 for 24 h. The results are shown as induction factor. *Bars,* SEM. The expressed proteins were detected using the anti-flag M2 antibody after 1 h of hormone stimulation. *D,* the expression plasmids for WT and Δ11 were transfected into PC3 cells together with PSA promoter luciferase reporter. The cells were stimulated for 24 h with different concentrations of 5α-dihydrotestosterone (*5α-DHT*), with or without Casodex (1 μmol/L). Results are shown as induction factor. *Bars,* SEM.

(21). ΔFQNLF/Δ1, ΔFQNLF/Δ11, ΔFQNLF/R629Q, and ΔFQNLF/K630T were created by exchanging *Hin*dIII/*Psy*I fragments.

Cell culture, transient transfections, luciferase, and β-galactosidase assays. HeLa, COS, and PC3 cells were obtained from the American Type Culture Collection and cultured as described before (36, 39). The T-REX-TAT GRE cell line was established by the integration of a pcDNA5/FRT/TO–derived vector into the 293 Flp-In cell line according to the manufacturer's instruction (Invitrogen). The pcDNA5/FRT/TO–derived vector contains the pGL4 *luciferase* gene (Promega) regulated by the E1B TATA box and two copies of the TAT GRE and is flanked by two chicken β-globin insulators.

Cells were transfected as described using a mixture of 100 ng luciferase reporter plasmid and 10 ng pCMV-β-gal plasmid as an internal control (36). Various amounts of full-length AR expression plasmids (10 ng), GAL4 fusion plasmid (50 ng), and VP16 fusion plasmid (50 ng) were cotransfected. The T-REX-TAT GRE cell line was transfected with 10 ng of pCMV-β-gal plasmid and 50 ng of AR expression plasmids. After overnight incubation, the medium was replaced and cells were stimulated with either the synthetic androgen methyltrienolone (R1881, Perkin-Elmer Life Sciences), 5α-dihydrotestosterone (Sigma), or testosterone (Sigma) at concentrations mentioned in the legends of the figures. The antiandrogen casodex was supplied by AstraZeneca Pharmaceuticals. Twenty-four hours after

stimulation, cells were lysed in 25 μL passive lysis buffer (Promega). The luciferase and β-galactosidase activities were measured and calculated as described (36). Induction factors represent the luciferase activity of hormone-stimulated cells relative to the activity of nonstimulated cells. The values shown are the averages of at least three independent experiments done in duplicate. The error bars are the SEMs.

Immunoblotting. For immunoblotting, HeLa cells were plated into a 24-well plate (62,000 per well) and transfected with 500 ng expression plasmid. The proteins were detected with a monoclonal antibody against the flag epitope (M2 antibody). Details of the immunoblotting experiments were described elsewhere (21).

Immunocytofluorescence staining and fluorescence microscopy. HeLa cells were plated into chambered cover glass Labtek 4-well slides (Sanbio; 60,000 per well) and transfected with 500 ng of either EGFP-WT, EGFP-hinge mutants, SV40NLS, or SV40NLS-Δ11 expression plasmid using GeneJuice transfection reagent as described above. Cells were stimulated for 1 h with 10 nmol/L R1881. The SV40NLS-WT and SV40NLS-Δ11 proteins were immunostained with an M2 anti-flag antibody (Stratagene) followed by incubations with tetramethyl rhodamine isothiocyanate–conjugated goat anti-mouse antibody (Sigma-Aldrich). The subcellular distribution of the expressed proteins was analyzed by fluorescence microscopy using a Nikon Diaphod inverted microscope.

Bandshift experiments. For the bandshift experiments, whole-cell extracts of COS cells containing human AR or derived mutants were used. COS cells were plated in 6-cm Petri dishes (600,000 per dish) and transfected with 3 μg of expression plasmid. The transfected cells were stimulated with 10 nmol/L R1881 for 1 h, washed twice with 1 mL ice-cold PBS, and harvested in 500 μL PBS. Whole-cell extracts were prepared by adding 50 μL extraction buffer [20 mmol/L HEPES-KOH (pH 7.8), 450 mmol/L NaCl, 0.4 mmol/L EDTA, 25% glycerol, 0.5 mmol/L DTT, and 0.5 mmol/L phenylmethylsulfonyl fluoride]. The cells were lysed by freezing-thawing thrice using liquid N_2 and ice. The cell debris was removed by a 10-min centrifugation at 20,000 × *g*. The bandshift experiments were done with ~5 μg extract as described earlier (36), and for supershift experiments 0.3 μL of homemade antibody against the first 21 residues against the human AR was added.

Results

Functional analysis of two prostate cancer mutations in the *AR* gene. Two point mutations in the hinge region of the AR, resulting in substitutions R629Q and K630T, have been reported in biopsies of prostate cancer (6, 7). The effect of these substitutions on the functionality of the AR was investigated. Both R629Q and K630T substitution mutants show a higher transcriptional potency but not a higher efficacy (Fig. 1*A*). Although R629 and K630 are located within the CTE that is involved in DNA binding, *in vitro* bandshift experiments reveal that neither mutation affects DNA binding (Fig. 1*B*). These two mutated residues also lie within the NLS of the AR. Using fluorescence microscopy, the possible effects of these mutations on intracellular localization of EGFP fusion proteins was

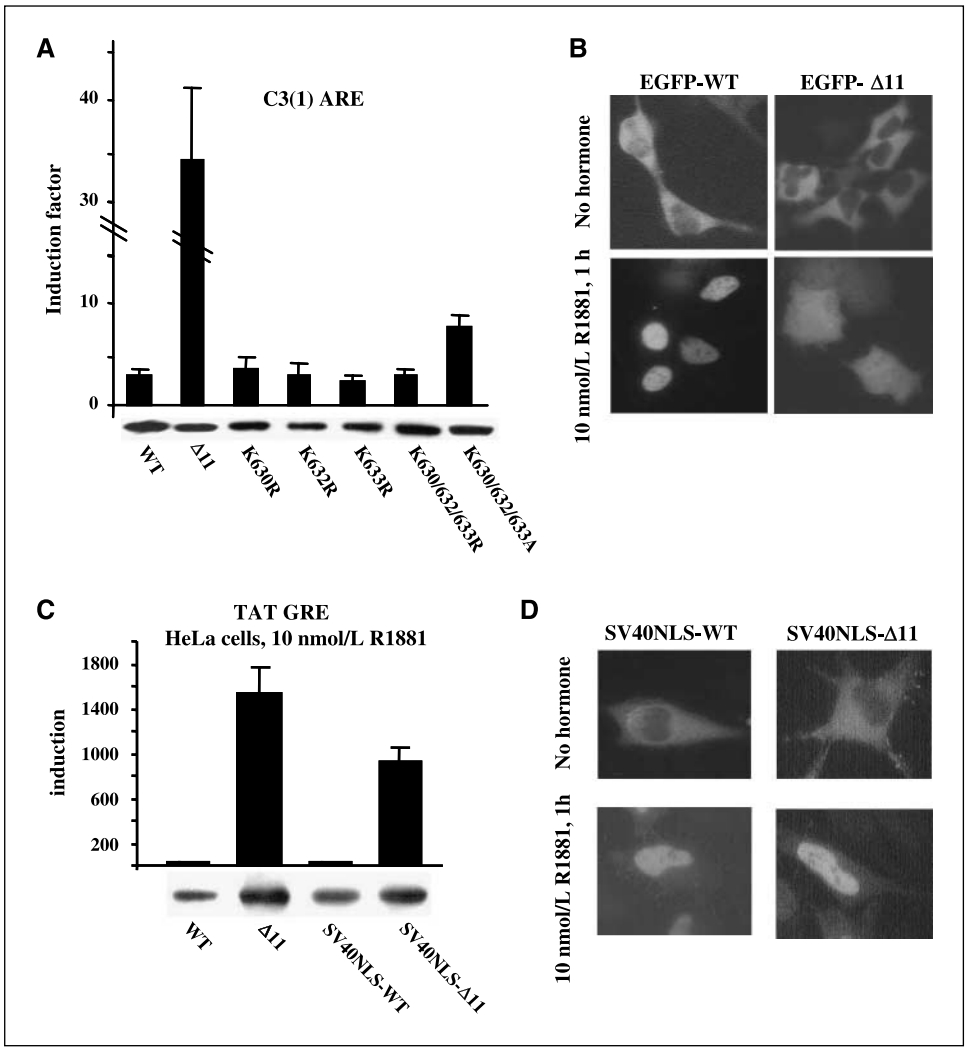

Figure 3. The inhibitory region coincides with the acetylation sites and the NLS. *A,* expression plasmids were transfected into HeLa cells together with the C3(1) ARE luciferase reporter. The cells were stimulated for 24 h with 10 nmol/L R1881. Results are shown as induction factor. *Bars,* SEM. For immunoblotting, transfected HeLa cells were stimulated for 1 h with 10 nmol/L R1881. The expressed proteins were detected using the anti-flag M2 antibody. *B,* fluorescence microscopy. HeLa cells were transfected with either EGFP-WT or EGFP-Δ11 expression plasmid. The subcellular distribution of the EGFP fusion proteins without hormone and after 1-h stimulation with 10 nmol/L R1881 was analyzed by fluorescence microscopy. *C,* functional analysis of the SV40NLS fusions. Expression plasmid for the WT, Δ11, and the respective SV40NLS fusions were transfected in HeLa cells together with the TAT GRE reporter. The cells were stimulated for 24 h with 10 nmol/L R1881. *D,* immunocytofluorescence staining. HeLa cells were transfected with either SV40NLS-WT or SV40NLS-Δ11 expression plasmid. The expressed proteins were immunostained and analyzed by fluorescence microscopy.

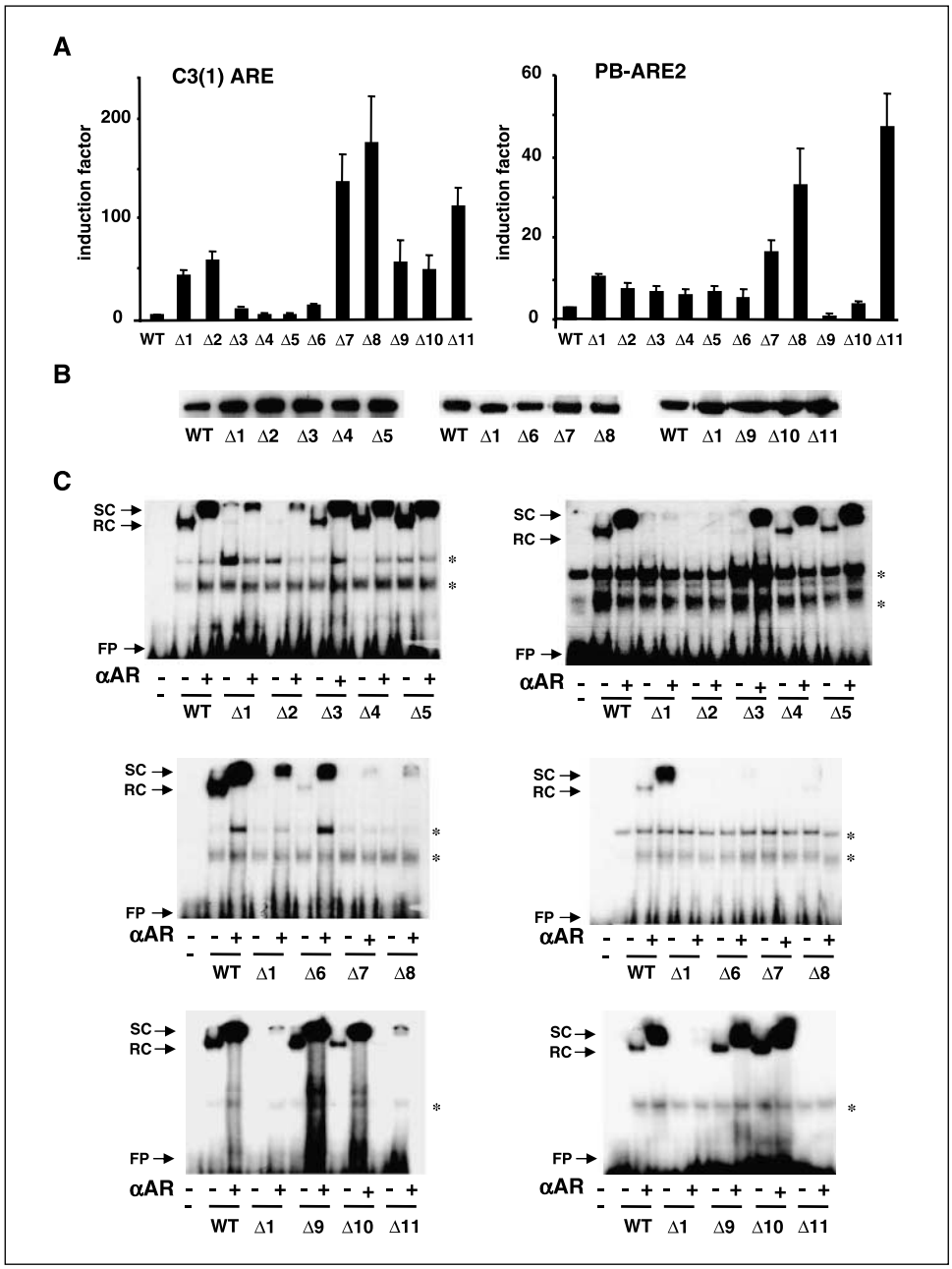

Figure 4. Functional and DNA-binding analysis of full-length deletion mutants using a nonselective and an androgen-selective ARE. *A,* transfection experiments. The expression plasmids were transfected into HeLa cells together with either the nonselective C3(1) ARE or the androgen-selective PB-ARE2 luciferase reporter. The cells were stimulated for 24 h with 10 nmol/L R1881. Results are shown as induction factor. *Bars,* SEM. *B,* immunoblotting. COS cells were transfected and stimulated for 1 h with 10 nmol/L R1881. Whole-cell extracts were made and immunoblotted. The expressed proteins were detected using the anti-flag M2 antibody. *C,* bandshift experiments. Labeled C3(1)ARE or PB-ARE2 probe was incubated with whole-cell extracts containing the indicated proteins. No protein was added to the first lanes as a negative control. The supershifts were obtained by adding a specific antibody against AR. *Arrows,* the positions of the free unbound probe (*FP*), the retarded complex (*RC*), and the supershifted complex (*SC*). *, nonspecific complexes.

evaluated (Fig. 1*C*). In the absence of hormone, all EGFP fusions show a mainly cytoplasmic distribution. After 1 h of hormone stimulation, EGFP-WT is exclusively nuclear, whereas EGFP-R629Q and EGFP-K630T show incomplete nuclear translocation.

Identification and delineation of an inhibitory region. The fact that two point mutations in the hinge region affect the AR activity prompted a thorough analysis of this region. The transactivation potential of Δ1, an AR deleted of residues 628 to 646, was increased compared with WT AR (Fig. 2*A*). Expression of WT and Δ1 proteins was checked by immunoblotting. To delineate the inhibitory region, a deletion analysis was done both at the NH_2-terminal (Δ2-Δ5) and at the COOH-terminal (Δ6–Δ8) border of the region of interest. The resulting constructs are represented in Fig. 2*A* and their activity was compared in transfection assays. The Δ1 and Δ2 constructs show an increased potency. Smaller NH_2-terminal deletions (Δ3–Δ5) resulted in receptor constructs with induction factors similar to WT AR. The constructs with COOH-terminal deletions starting at residue 628 (Δ6–Δ8) mediate higher induction factors. Although both Δ9 and Δ10 show increased transcriptional activity, the minimal deletion that resulted in the most potent receptor (Δ11) was from position 629 to 636. In conclusion, the motif spanning amino acids 629 to 636 (RKLKKLGN) in the hinge region of the human AR limits its transcriptional activity.

The hormone sensitivity of the Δ11 construct was evaluated on the TAT GRE reporter by an activation assay at increasing hormone concentrations (Fig. 2*B*). At low hormone concentrations, Δ11 is less active that WT, whereas at higher concentrations the luciferase activity induced by Δ11 is up to 30-fold higher. In addition, the Δ11 mutant is more active than WT on a chromatin-integrated reporter (Fig. 2*C*). In the prostate cancer cell line PC3, the transcriptional

response of the human PSA promoter was determined for the WT and Δ11 proteins. Once again, Δ11 displays superactivity in response to testosterone, 5α-dihydrotestosterone, and R1181 (Fig. 2*D*, and data not shown). This superactivity can be efficiently blocked by casodex.

The acetylation sites and the NLS coincide with the inhibitory region. Acetylation of the AR has been reported on lysines 630, 632, and 633 (Fig. 2*A*; refs. 30–33). All three residues are located within the inhibitory region and one of the three is mutated in the prostate cancer mutant K630T. A potential role of these acetylations in the inhibitory control of the hinge region was studied by mutating them into arginine or alanine. A mutation of a lysine into an arginine prevents possible acetylation but retains the basic character of the residue, whereas mutation into an alanine eliminates both properties. All constructs show a transcriptional activity comparable with the WT AR, except the K630/632/633A mutant, which is ~2-fold more active (Fig. 3*A*).

Besides the acetylation sites, the inhibitory region also partially overlaps with the bipartite NLS (Fig. 2*A*; ref. 29). As expected, deletion of the inhibitory region impairs the hormone-dependent nuclear translocation. However, a terminally fused SV40 NLS restores the hormone-dependent nuclear translocation but does not affect the superactivity of the Δ11 construct (Fig. 3).

DNA binding by the AR deletion mutants. Because the inhibitory region overlaps with the earlier-described CTE that is involved in DNA recognition by the AR-DBD, we evaluated the DNA-binding capacities of the AR deletion mutants Δ1 to Δ11. The functional activity of Δ1 to Δ11 was tested on reporter constructs based on the nonselective C3(1) ARE and the androgen-selective PB-ARE-2 (Fig. 4*A*). Comparison with the results of the MMTV promoter (Fig. 2*A*) reveals no major differences, although the PB-ARE-2 reporter seems less responsive to superactivation compared with the C3(1) ARE reporter.

The DNA binding of the AR mutants was tested in bandshift experiments with the C3(1) ARE and the PB-ARE-2 as DNA probe (Fig. 4). The largest deletion in the hinge (Δ1) diminishes the affinity for both probes. Increasing the length of the CTE (Δ2–Δ5) improved DNA binding, with the most pronounced effect for the C3(1) ARE. Stepwise deletions in the NH_2-terminal part of the CTE (Δ6–Δ8) seems to destroy DNA binding to the PB-ARE2, whereas only Δ6 binds to the C3(1) ARE. The Δ9 and Δ10 constructs show WT DNA-binding characteristics, probably because of the similarity between the remaining residues after deletion; however, Δ11 gives the same results as Δ1.

AF1 and AF2 of the AR mutant. For most nuclear receptors, two AFs have been characterized, AF1 in the NTD and AF2 in the LBD. The following experiments were designed to check whether the hinge affects AF1, AF2, or both. GAL4 DBD fusions with AR-LBDs (Fig. 5*A*) were developed to avoid any effects on DNA binding and nuclear translocation via the AR-DBD that may have occurred as a result of deletion of amino acids in the CTE. When comparing the transcriptional activity of the WT/ΔAF2 protein with that of the mutant Δ1/ΔAF2 protein, no inhibitory effect of the hinge region on AF1 could be observed.

Next, we tried to determine whether the hinge region has an effect on AF2. The AR DBD-hinge-LBD fragments were fused to the

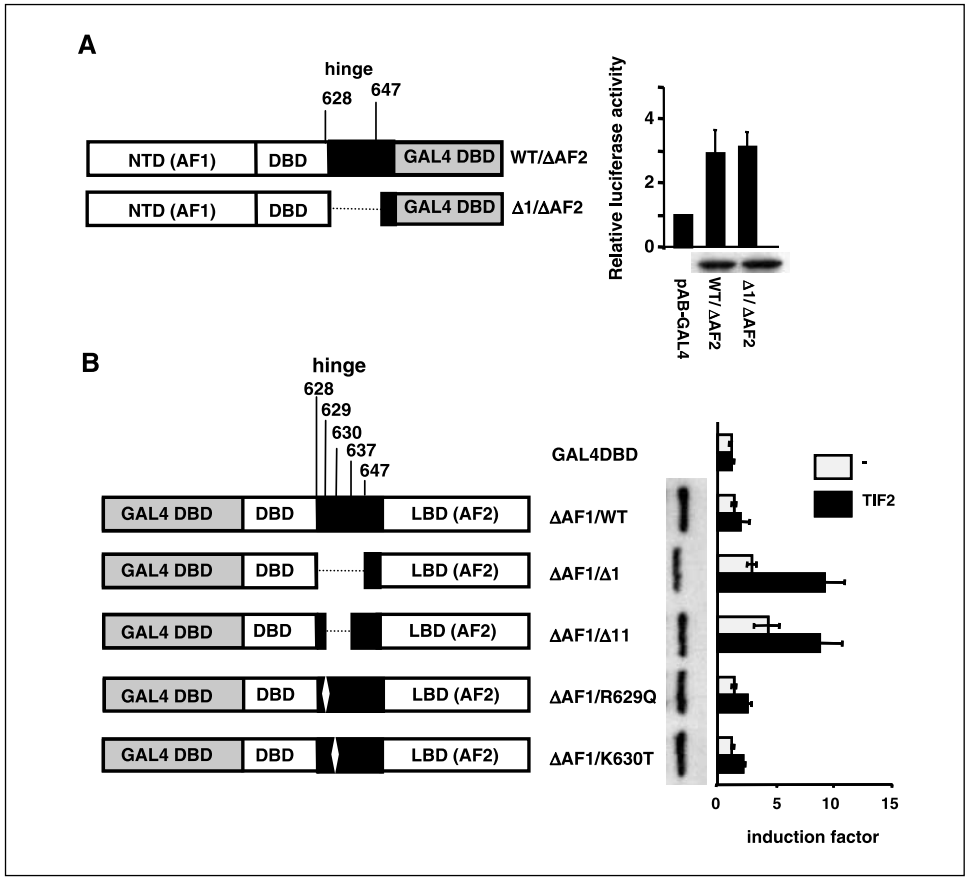

Figure 5. Effect of the hinge region on AF1 and AF2. *A,* schematic representation and functional test of WT/ΔAF2 and Δ1/ΔAF2. HeLa cells were transfected with the $(GAL)_5$TATA-luc reporter construct and the respective expression plasmids, in which the pAB-GAL4 plasmid was used as a reference control. The results are shown as luciferase activity of WT/ΔAF2 and Δ1/ΔAF2 relative to the pAB-GAL4. *Bars,* SEM. Expression was checked by immunoblotting. *B,* schematic representation and functional test of ΔAF1/WT and ΔAF1 mutants. HeLa cells were transfected with the $pUAS_4$TATA-luc reporter construct and the respective expression plasmids, with or without the expression plasmid for the coactivator TIF2. The pAB-GAL4-flag plasmid was used as a reference control. The cells were stimulated for 24 h with 10 nmol/L R1881. Results are shown as induction factor. *Bars,* SEM. Expression was checked by immunoblotting.

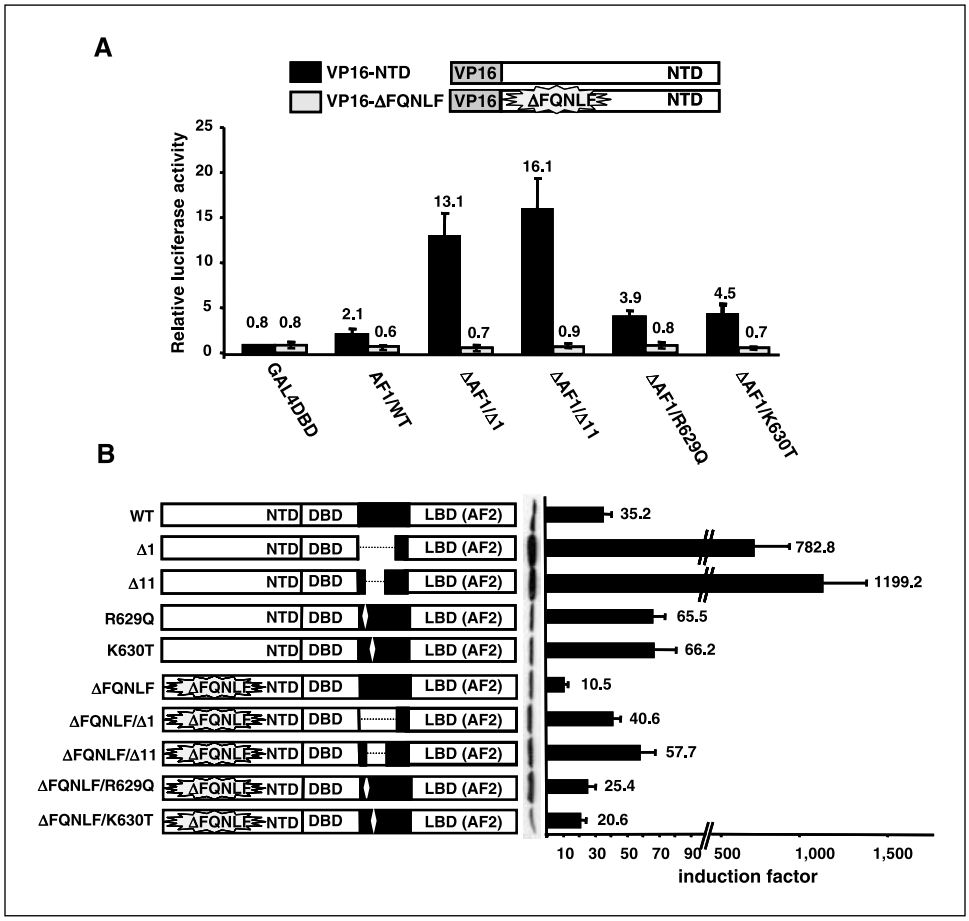

Figure 6. Effect of the hinge region on N/C interaction. *A,* N/C interaction in mammalian double-hybrid. HeLa cells were transfected with the indicated expression plasmid and the $(GAL)_5$TATA-luc construct. The cells were stimulated for 24 h with 10 nmol/L R1881. The results are shown as relative luciferase activity representing the luciferase activity of cells cotransfected with either the VP16-NTD or the VP16-ΔFQNLF construct, relative to the activity of cells cotransfected with VP16. *Bars,* SEM. *B,* N/C interaction in the context of the full-size AR. HeLa cells were transfected with the indicated expression plasmid and androgen-responsive TAT-GRE reporter. The cells were stimulated for 24 h with 10 nmol/L R1881. The results are shown as induction factor. *Bars,* SEM. For immunoblotting, the expression plasmids were transfected into HeLa cells. The cells were stimulated for 1 h with 10 nmol/L R1881. The expressed proteins were detected using the anti-flag M2 antibody.

heterologous GAL4 DBD (Fig. 5*B*). The ΔAF1/WT construct is inactive. Although the mutant ΔAF1/Δ1 and ΔAF1/Δ11 constructs have moderate transcription activity, no induction could be observed with the prostate cancer mutations. Because AF2 activity is normally dependent on the recruitment of coactivators, we cotransfected the p160 coactivator, TIF2, with each of the ΔAF1 constructs. In the absence of the hinge region (ΔAF1/Δ1 and ΔAF1/Δ11), AF2 was coactivated by TIF2 under conditions in which almost no coactivation was seen for the WT or the prostate cancer mutants.

The N/C interactions in the hinge mutants. The role of the hinge region on the N/C interaction was tested in a mammalian double-hybrid assay (Fig. 6*A*). ΔAF1/WT and the corresponding hinge mutants depicted in Fig. 5*B* were coexpressed with the WT NTD fused with the VP16 protein. The resulting luciferase values for the ΔAF1/Δ1 and ΔAF1/Δ11 double hybrids are 6- to 7-fold higher than those for ΔAF1/WT, indicating a much stronger N/C interaction in the absence of the inhibitory hinge region. Similarly, the prostate cancer mutants also showed an increased N/C interaction, although to a much lower extent. The VP16-NTD fusion deleted of the 23-FQNLF-27 motif has a deficient N/C interaction, as described earlier (21).

Subsequently, we investigated the N/C interaction in the context of the full-length AR. The transcriptional activities of the WT, Δ1, Δ11, R629Q, and K630T constructs were compared in the absence or presence of the 23-FQNLF-27 motif (Fig. 6*B*). The data confirm the results of the double-hybrid assays because the superactivities of the Δ1 and Δ11 constructs drop considerably when the 23-FQNLF-27 motif was deleted. For the prostate cancer mutants, again a similar but less profound effect is observed. After deletion of the 23-FQNLF-27 motif, and hence in the absence of a N/C interaction (21), the superactivation due to the hinge mutations diminishes considerably, but is not completely abolished.

Discussion

Role of hinge region mutations in prostate cancer. The AR plays a key role in the development of prostate cancer and in resistance to hormone therapy (2, 3). Several point mutations in and around the hinge region have been identified in prostate cancer patients (6–11). In our assays, both the R629Q and the K630T mutants (6, 7) have an increased potency (Fig. 1*A*). Another mutation, S646F, was identified in a patient with a very rapid relapse after hormone therapy and was also shown to result in a higher androgen response (10). The fact that prostate cancer mutations in the hinge region show increased transcriptional responses is an indication for an inhibitory function of this domain. Because an aberrant AR activity might be a key in the development of prostate cancer (4), it is of major interest to have an in-depth knowledge of the regulation of the AR and the role of the hinge herein. Therefore, we did a functional analysis of the hinge region of the AR.

The hinge region attenuates the transcriptional activity of the AR. A human AR with a deletion of the residues 628 to 646 in the hinge region (Δ1) mediates an increased androgen response (Fig. 2*A*). This is in agreement with different initial reports (40–42).

We delineated the part of the hinge that inhibits the transcriptional activity of the full-length human AR to a highly basic motif between residue 629 and 636 (629-RKLKKLGN-636; Fig. 2*A*). The fact that this motif is conserved in all known AR sequences is an indication for its functional importance. The inhibitory effect of the hinge is not promoter specific and occurs both on naked as well as on chromatinized templates.

The hinge region contains a PEST sequence that is presumed to regulate ubiquitylation (43). This element is partially deleted in the Δ1 construct. When the complete PEST sequence (residues 639–657) was deleted, no effects were observed on the activity or the expression of the AR (data not shown). This implies that the superactivity of the hinge deletion mutants is not due to an altered ubiquitylation.

Although Δ11 shows a much higher transactivation potential, there is no difference in efficacy (Fig. 2*B*). The weaker activity of Δ11 compared with WT in Fig. 2*B* at low hormone concentrations might result from the impaired nuclear translocation. The superactivity of Δ11 is also induced by the natural androgens testosterone and 5α-dihydrotestosterone (Fig. 2*C* and data not shown). We postulate that under normal physiologic conditions, the hinge is involved in an attenuating activity to avoid overactivity during hormone stimulation. We propose that mutations in the hinge region might result in a gain-of-function, resulting in a "super"-AR that can contribute to the development of prostate cancer and therapeutic relapse (2–5).

The basic residues in the hinge region are crucial for transcriptional control. The AR can be acetylated by p300, p/CAF, and Tip60 (30) in the hinge region at residues K630, K632, and K633 (30, 44). It was proposed that the acetylation site was a docking site for either coactivators or corepressors, and that acetylation of these lysine residues switches on the recruitment of such cofactors (31, 33). In our hands, preventing acetylation of the AR by mutating lysines into arginines at positions 630, 632, and 633 resulted in WT transcriptional activation potential in transfections (Fig. 3*A*). Even simultaneous mutation of all three lysines into arginines did not change the transactivation potential. Therefore, in our assays, acetylation of the 629-RKLKKLGN-636 motif probably does not play a major role in the inhibitory effect of the hinge on the AR activity. In contrast, the overall positive charge of the motif seems critical in the control of the AR activity. Indeed, substitutions that conserve the positive nature have no influence on transactivation, whereas substitutions attenuating the basic character increase the transcriptional activity.

We assume that the high-level activity of Δ1 or Δ11 is not reached by substitution mutations because the remaining residues can rescue the effect of the lost positive residues. The NH_2-terminal parts of the hinge regions of the other steroid receptors also have a highly basic character. It would be interesting to investigate whether these have a similar inhibitory effect on transactivation. The positive residues might form a docking site for the recruitment of repressing proteins. This idea is strengthened by the fact that an amphipathic α-helix with a hydrophobic and a positive side is predicted by Predictprotein[1] between residues G627 and N636. Several inhibitory proteins have been identified that interact with the hinge, for example, FLNa (45), SMRT (46), ARR19 (47), and Pod-1 (48). It would be interesting to test whether the hinge plays a role in the recruitment of these or other regulatory factors. In conclusion, our results do not match the model in which mutations that knockout possible acetylation sites attenuate the activity and mutations that mimic acetylation increases the activity (33). However, our data fit with another report that mentions an AR mutant deleted of the acetylation sites (residues 629–633), which is transcriptionally more active (49).

The superactivity is independent of nuclear translocation. Unliganded AR resides largely in the cytoplasm, but translocates to the nucleus upon hormone binding. This nuclear transport is complete 15 to 60 min after hormone stimulation (50). The AR has a NLS (617-RKCYEAGMTLGA**RK**LKK-633) consisting of two clusters of basic residues (underlined), which are localized in the DBD and the hinge, respectively (29). The two prostate cancer hinge mutations are within the second half of the NLS (indicated in bold). The hormone-dependent nuclear translocation of the mutant EGFP-R629Q and EGFP-K630T proteins is partially impaired (Fig. 1*D*), as is the case for the EGFP-Δ11 mutant (Fig. 3*B*). The impaired nuclear translocation is in seeming contradiction with the enhanced androgen response mediated by the mutations in the hinge region. In addition, restoring the hormone-dependent nuclear translocation by adding an SV40NLS still results in a superactive receptor after deletion of the inhibitory region (Fig. 3*C* and *D*). This implies that there is no strict correlation between impaired nuclear translocation and enhanced transactivation.

Inverse correlation between DNA-binding affinity and transactivation potential. The androgen and glucocorticoid receptors bind very similar DNA sequences. However, in addition to the nonselective hormone response elements, there exist androgen-selective AREs, recognized by the AR but not by the glucocorticoid receptor. The AR-DBD requires a CTE of at least four residues (625-TLGA-628) for proper DNA binding to nonselective AREs and a CTE of at least 12 residues (625-TLGA**RK**LKKLGN-636) for binding to androgen-selective AREs (25–28). The two prostate cancer mutations (indicated in bold) are localized in this CTE; however, DNA binding is not affected by the R629Q and K630T substitutions (Fig. 1*C*).

The inhibitory motif 629-RKLKKLGN-636 coincides with the last eight residues of the CTE necessary for proper DNA binding by isolated AR-DBD constructs (25). AR deletions affecting this CTE also result in a weaker DNA binding by the full-size AR, especially for the androgen-selective AREs (Fig. 4*C, right*). Most surprisingly, mutants that weakly bind DNA show high hormone-induced transcriptional activity (Figs. 2*A* and 4*A*). In fact, there seems to be an inverse correlation between affinity for DNA and transactivation.

Implications of the hinge region in AF1 and AF2. Although the AR is a member of the superfamily of the nuclear receptors, it has several specific features. One such feature is that the AR exhibits a very weak AF2 and a very strong AF1 activity (19, 50). This is explained, in part, by the fact that the NTD is the major recruitment domain for the p160 coactivators (16, 17, 19). Inactivating mutations in the two transcription activating units of AF1 (Tau-1 and Tau-5) almost completely inactivates the AR, indicating that AF2 has little activity (39). By consequence, it was surprising that the hinge had no effect on the AF1 (Fig. 5*A*). The deletion of the hinge resulted in a small increase of the isolated AF2, and cotransfection of TIF2 enhanced this activity further in absence of the hinge region (Fig. 5*B*). Therefore, in agreement with other reports (41), we observed that the hinge region seems to have

[1] http://cubic.bioc.columbia.edu/predictprotein/

an attenuating effect on AF2, possibly through an interference with coactivator recruitment.

Deletion of the hinge region enhances the N/C interaction. The intramolecular N/C interaction between the 23-FQNLF-27 motif in the NTD and the AF2 coactivator binding pocket of the LBD has functional importance to ligand binding and transactivation (21, 22). Δ11 shows an increased N/C interaction as well as a higher transcriptional activity on a stably integrated reporter (Fig. 2*C*). This is in agreement with the results of Li et al. (23), who described the necessity of the FQNLF motif for activation of chromatin-based templates. Moreover, we even observed a stronger N/C interaction when the hinge region is mutated (Fig. 6*A*). The transactivation potential of the full-size AR drops ~3-fold when the N/C interaction is abolished (Fig. 6*B*). By contrast, the activity of the Δ11 construct drops even more than 20-fold. However, even with a disrupted N/C interaction, superactivation is observed after deletion of the inhibitory region. Probably, these effects are explained by the fact that the deletion of the inhibitory region increases the affinity of the AF2 for all binding partners such as the NTD, TIF2, and other coactivators.

In conclusion, the analysis of two point mutations indicates that the hinge region is of major importance for the regulation of AR activity. Some mutations result in an AR that is hyperactive, which strongly contrasts to a decreased nuclear localization and DNA binding. We even observed increased transactivation by mutant ARs for which no DNA binding is observed in bandshift assays. Taken together, the hinge region is implicated in several AR features, such as nuclear localization, DNA binding, coactivator recruitment, and N/C interaction, which contribute to the overall function of the AR. Mutations in this region can thus result in an aberrant androgen response that might be involved in the development of prostate cancer.

Acknowledgments

Received 5/10/2006; revised 1/29/2007; accepted 2/15/2007.

Grant support: Geconcerteerde Onderzoeksactie van de Vlaamse Gemeenschap, "Fonds voor Wetenschappelijk Onderzoek-Vlaanderen" grant 1.5.065.05, and the Congressionally Directed Medical Research Program (Prostate Cancer Research Program award DAMD17-02-1-0082).

The costs of publication of this article were defrayed in part by the payment of page charges. This article must therefore be hereby marked *advertisement* in accordance with 18 U.S.C. Section 1734 solely to indicate this fact.

We thank R. Bollen, H. Debruyn, and K. Bosmans for their excellent technical assistance, and our colleagues at the Molecular Endocrinology Laboratory for helpful discussions.

References

1. Quigley CA, De Bellis A, Marschke KB, El-Awady MK, Wilson EM, French FS. Androgen receptor defects: historical, clinical, and molecular perspectives. Endocr Rev 1995;16:271–321.
2. Linja MJ, Visakorpi T. Alterations of androgen receptor in prostate cancer. J Steroid Biochem Mol Biol 2004;92:255–64.
3. Chen CD, Welsbie DS, Tran C, et al. Molecular determinants of resistance to antiandrogen therapy. Nat Med 2004;10:33–9.
4. Taplin M-E, Balk SP. Androgen receptor: a key molecule in the progression of prostate cancer to hormone independence. J Cell Biochem 2004;91:483–90.
5. Isaacs JT, Isaacs WB. Androgen receptor outwits prostate cancer drugs. Nat Med 2004;10:26–7.
6. Wang C, Uchida T. Androgen receptor gene mutations in prostate cancer. Jpn J Urol 1997;88:550–6.
7. Tilley WD, Buchanan G, Hickey TE, Bentel JM. Mutations in the androgen receptor gene are associated with progression of human prostate cancer to androgen independence. Clin Cancer Res 1996;2:277–85.
8. Buchanan G, Yang M, Harris JM, et al. Mutations at the boundary of the hinge and ligand binding domain of the androgen receptor confer increased transactivation function. Mol Endocrinol 2001;15:46–56.
9. Céraline J, Cruchant MD, Erdmann E, et al. Constitutive activation of the androgen receptor by a point mutation in the hinge region: a new mechanism for androgen-independent growth in prostate cancer. Int J Cancer 2004;108:152–7.
10. Thompson J, Hyytinen ER, Haapala K, et al. Androgen receptor mutations in high-grade prostate cancer before hormonal therapy. Lab Invest 2003;83:1709–13.
11. Taplin ME, Bubley GJ, Shuster TD, et al. Mutation of the androgen-receptor gene in metastatic androgen-independent prostate cancer. N Engl J Med 1995;332:1393–8.
12. Robinson-Rechavi M, Escriva Garcia H, Laudet V. The nuclear receptor superfamily. J Cell Sci 2003;116:585–6.
13. Aranda A, Pascual A. Nuclear hormone receptors and gene expression. Physiol Rev 2001;81:1269–304.
14. Schaufele F, Carbonell X, Guerbadot M, et al. The structural basis of androgen receptor activation: intramolecular and intermolecular amino-carboxy interactions. Proc Natl Acad Sci U S A 2005;102:9802–7.
15. Heinlein CA, Chang C. Androgen receptor (AR) coregulators: an overview. Endocr Rev 2002;23:175–200.
16. Christiaens V, Bevan CL, Callewaert L, et al. Characterization of the two coactivator-interacting surfaces of the androgen receptor and their relative role in transcriptional control. J Biol Chem 2002;277:49230–7.
17. Bevan C, Hoare S, Claessens F, Heery DM, Parker MG. The AF1 and AF2 domains of the androgen receptor interact with distinct regions of SRC1. Mol Cell Biol 1999;19:8383–92.
18. Berrevoets CA, Doesburg P, Steketee K, Trapman J, Brinkmann AO. Functional interactions of the AF-2 activation domain core region of the human androgen receptor with the amino-terminal domain and with the transcriptional coactivator TIF2 (transcriptional intermediary factor 2). Mol Endocrinol 1998;12:1172–83.
19. Alen P, Claessens F, Verhoeven G, Rombauts W, Peeters B. The androgen receptor amino-terminal domain plays a key role in p160 coactivator-stimulated gene transcription. Mol Cell Biol 1999;19:6085–97.
20. He B, Kemppainen JA, Voegel JJ, Gronemeyer H, Wilson EM. Activation function 2 in the human androgen receptor ligand binding domain mediates interdomain communication with the NH_2-terminal domain. J Biol Chem 1999;274:37219–25.
21. Callewaert L, Verrijdt G, Christiaens V, Haelens A, Claessens F. Dual function of an amino-terminal amphipatic helix in androgen receptor-mediated transactivation through specific and nonspecific elements. J Biol Chem 2003;278:8212–8.
22. He B, Kemppainen JA, Wilson EM. FXXLF and WXXLF sequences mediate the NH_2-terminal interaction with the ligand binding domain of the androgen receptor. J Biol Chem 2000;275:22986–94.
23. Li J, Fu J, Toumazou C, Yoon H-G, Wong J. A role of the amino-terminal (N) and carboxyl-terminal (C) interaction in binding of androgen receptor to chromatin. Mol Endocrinol 2006;20:776–85.
24. Khorasanizadeh S, Rastinejad F. Nuclear-receptor interactions on DNA-response elements. Trends Biochem Sci 2001;26:384–90.
25. Schoenmakers E, Alen P, Verrijdt G, et al. Differential DNA binding by the androgen and glucocorticoid receptors involves the second Zn-finger and a C-terminal extension of the DNA-binding domains. Biochem J 1999;341:515–21.
26. Claessens F, Verrijdt G, Schoenmakers E, et al. Selective DNA binding by the androgen receptor as a mechanism for hormone-specific gene regulation. J Steroid Biochem Mol Biol 2001;76:23–30.
27. Haelens A., Verrijdt G, Callewaert C, et al. DNA recognition by the androgen receptor: evidence for an alternative DNA-dependent dimerization, and an active role of sequences flanking the response element. Biochem J 2003;369:141–51.
28. Verrijdt G, Haelens A, Claessens F. Selective DNA recognition by the androgen receptor as a mechanism for hormone-specific regulation of gene expression. Mol Genet Metab 2003;78:175–85.
29. Zhou ZX, Sar M, Simental JA, Lane MV, Wilson EM. A ligand-dependent bipartite nuclear targeting signal in the human androgen receptor. Requirement for the DNA-binding domain and modulation by NH_2-terminal and carboxyl-terminal sequences. J Biol Chem 1994;269:13115–23.
30. Fu M, Wang C, Reutens AT, et al. p300 and p300/cAMP-response element-binding protein-associated factor acetylate the androgen receptor at sites governing hormone-dependent transactivation. J Biol Chem 2000;275:20853–60.
31. Fu M, Wang C, Wang J, et al. Androgen receptor acetylation governs *trans* activations and MEKK1-induced apoptosis without affecting *in vitro* sumoylation and *trans*-respression function. Mol Cell Biol 2002;22:3373–88.
32. Thomas M, Dadgar N, Aphale A, et al. Androgen receptor acetylation site mutations cause trafficking defects, misfolding, and aggregation similar to expanded glutamine tracts. J Biol Chem 2004;279:8389–95.
33. Fu M, Rao M, Wang C, et al. Acetylation of androgen receptor enhances coactivator binding and promotes prostate cancer cell growth. Mol Cell Biol 2003;23:8563–75.
34. Green S, Issemann I, Sheer E. A versatile *in vivo* and *in vitro* eukaryotic expression vector for protein engineering. Nucleic Acids Res 1988;16:369.
35. Schoenmakers E, Verrijdt G, Peeters B, Verhoeven G, Rombauts W, Claessens F. Differences in DNA binding characteristics of the androgen and glucocorticoid receptors can determine hormone-specific responses. J Biol Chem 2000;275:12290–7.
36. Haelens A, Verrijdt G, Callewaert L, Peeters B, Rombauts W, Claessens F. Androgen-receptor-specific DNA binding to an element in the first exon of the human secretory component gene. Biochem J 2001;353:611–20.
37. Verrijdt G, Haelens A, Schoenmakers E, Rombauts W, Claessens F. Comparative analysis of the influence of the high-mobility group box 1 protein on DNA binding and

transcriptional activation by the androgen, glucocorticoid, progesterone and mineralocorticoid receptors. Biochem J 2002;361:97–103.
38. Moehren U, Dressel U, Reeb CA, et al. The highly conserved region of the co-repressor Sin3A functionally interacts with the co-repressor Alien. Nucleic Acids Res 2004;32:2995–3004.
39. Callewaert L, Van Tilborgh N, Claessens F. Interplay between two hormone-independent activation domains in the androgen receptor. Cancer Res 2006;66:543–53.
40. Moilanen A, Rouleau N, Ikonen T, Palvimo JJ, Janne OA. The presence of a transcription activation function in the hormone-binding domain of androgen receptor is revealed by studies in yeast cells. FEBS Lett 1997;412:355–8.
41. Wang Q, Lu J, Yong EL. Ligand- and coactivator-mediated transactivation function (AF2) of the androgen receptor ligand-binding domain is inhibited by the cognate hinge region. J Biol Chem 2001;276:7493–9.
42. Tanner T, Claessens C, Haelens A. The hinge region of the androgen receptor plays a role in proteasome-mediated transcriptional activation. Ann N Y Acad Sci 2004;1030:587–92.
43. Sheflin L, Keegan B, Zhang W, Spaulding SW. Inhibiting proteasomes in human HepG2 and LNCaP cells increases endogenous androgen receptor levels. Biochem Biophys Res Commun 2000;276:144–50.
44. Gaughan L, Logan IR, Cook S, Neal DE, Robson CN. Tip60 and HDAC1 regulate androgen receptor activity through changes to the acetylation status of the receptor. J Biol Chem 2002;277:25904–13.
45. Loy CJ, Sim KS, Yong EL. Filamin-A fragment localizes to the nucleus to regulate androgen receptor and coactivator functions. Proc Natl Acad Sci U S A 2003;100:4562–7.
46. Liao G, Chen LY, Zhang A, et al. Regulation of androgen receptor activity by the nuclear receptor corepressor SMRT. J Biol Chem 2003;278:5052–61.
47. Jeong BC, Hong CY, Chattopadhyay S, et al. Androgen receptor corepressor-19 kDa (ARR19), a leucine-rich protein that represses the transcriptional activity of androgen receptor through recruitment of histone deacetylase. Mol Endocrinol 2004;18:13–25.
48. Hong CY, Gong EY, Kim K, et al. Modulation of the expression and transactivation of the androgen receptor by the basic helix-loop-helix transcription factor Pod-1 through recruitment of histone deacetylase 1. Mol Endocrinol 2005;19:2245–57.
49. Karvonen U, Janne OA, Palvimo JJ. Androgen receptor regulates nuclear trafficking and nuclear domain residency of corepressor HDAC7 in a ligand-dependent fashion. Exp Cell Res 2006;312:3165–83.
50. Tyagi RK, Lavrovsky Y, Ahn SC, Song CS, Chatterjee B, Roy AK. Dynamics of intracellular movement and nucleocytoplasmic recycling of the ligand-activated androgen receptor in living cells. Mol Endocrinol 2000;14:1162–74.